Impact of the Band Offset for n-Zn(O,S)/p-Cu(In,Ga)Se_2 Solar Cells

Samaneh Sharbati and James R. Sites

***Abstract*—The conduction-band offset (CBO) of the Zn(O, S)/Cu(In,Ga)Se_2 heterojunction can play a significant role in the performance of solar cells. The individual electron affinities and bandgaps are controlled by the oxygen-to-sulfur and gallium-to-indium ratios, and the resulting offsets can range from +1.3 eV in the "spike" direction to −0.7 eV in the "cliff" direction if the full range of the two ratios is considered. The optimal CBO of near +0.3 eV can be achieved with various combinations of the two ratios. The traditional CdS emitter is near optimal for the commonly used 1.15-eV Cu(In,Ga)Se_2 (CIGS) but less optimal for higher Ga. The flexibility with Zn(O,S) emitters ranging from above 90% oxygen for CIS down to 50% oxygen for CGS allows an optimal CBO over the full gallium range. Assuming that other factors remain constant, the optimal offset should also be able to reduce the loss in cell efficiency between room temperature and temperatures more typical of field conditions by about 1% absolute.**

***Index Terms*—CIGS solar cells, conduction band offset, efficiency.**

I. Introduction

THE use of Zn(O,S) buffer layers in place of CdS with Cu(In,Ga)Se_2 (CIGS) solar cells has been explored by many groups [1]–[3], and several have made respectable-efficiency cells [4], [5]. At least three deposition techniques, chemical-bath deposition (CBD) [6], atomic-layer deposition (ALD) [7], and magnetron sputtering [8] have been successful. The primary argument for the use of Zn(O,S) is that its higher bandgap, compared with CdS, allows for greater collection of short-wavelength photons [9]–[13]. A second reason, the focus of the work reported here, is that the conduction-band offset (CBO) can be tuned to a more optimal value through modification of the oxygen-to-sulfur ratio.

The CBO can compromise solar-cell performance for two very different reasons depending on its direction. If the resulting alignment produces what is commonly referred to as a "spike," and the spike is sufficiently large, photogenerated current is blocked, and efficiency rapidly approaches zero. On the other hand, the opposite alignment, generally called a "cliff," becomes a problem in forward bias and may significantly increase the interfacial recombination current, hence reducing the voltage and fill factor of the solar cell [14]. By common convention, the spike direction of band alignment is taken to be positive.

The optimal condition is a small positive offset [15], [16]. Gloeckler [17] showed that range of an optimal spike at room temperature is approximately +0.1 to +0.4 eV. Thus, it follows that any given buffer layer is well matched to a CIGS absorber only over a variation of 0.3 eV in the absorber's electron affinity. For CIGS, nearly all the variation in bandgap occurs in the conduction band [18], and hence, multiple buffer layers are necessary to cover the full 0.6-eV range in electron affinity.

CdS should be a well-matched buffer for CIGS gaps from approximately 1.05 to 1.35 eV, which spans the range of higher efficiency CIGS cells that have been reported. An important caveat, however, is that bandgap alignment is only one factor in determining a solar cell's performance. Hence, the optimal matches of Zn(O,S) and CIGS compositions calculated here implicitly assume that variations in other material properties do not overwhelm the band alignment considerations. Ultimately, of course, there will need to be an integration of all materials properties to fully explain the compositional variations in performance.

II. Band Variations

Fig. 1(a), based on [18, Tab. I], shows the conduction and valance energy band of CIGS as a function of Ga content. The bandgap in eV varies as

$$E_g(x) = 1.01 + 0.42x + 0.24x^2 \tag{1}$$

where x is the Ga anion fraction. The bandgap range is from 1.01 to 1.67 eV, and since the expansion is in the conduction band, the electron affinity must decrease by the same amount, reportedly from 4.35 to 3.69 eV [18], with a slight downward bowing in the conduction band. Fig. 1(b) shows the band variations for the Zn(O,S) system based on values determined by various groups [7], [19]–[22]. In this case, there is significant decrease in the energy of both bands as the oxygen fraction is increased. The bandgap variation of Zn(O,S) with oxygen fraction x, taken from [21], is approximately

$$E_g(x) = 3.6 - 0.4x - 3x(1-x) \tag{2}$$

where 3.6 eV is the ZnS gap and 3.2 eV the ZnO gap. In this case, the bowing factor is quite large. The bandgap is minimum where the sulfur and oxygen concentrations are nearly equal, and it increases with either a higher or lower oxygen ratio.

Manuscript received November 9, 2013; revised December 15, 2013; accepted December 27, 2013. Date of publication January 24, 2014; date of current version February 17, 2014. The work was supported in part by a subcontract from the U.S. National Renewable Energy Laboratory under an F-PACE Project funded by the U.S. Department of Energy's SunShot program.

S. Sharbati is with the Physics Department, Colorado State University, Fort Collins, CO 80523 USA, and also with the Department of Electrical Engineering, Ferdowsi University of Mashhad, Mashhad 91775 -1111, Iran (e-mail: samane.sharbati@gmail.com).

J. R. Sites is with the Physics Department, Colorado State University, Fort Collins, CO 80523 USA.

Digital Object Identifier 10.1109/JPHOTOV.2014.2298093

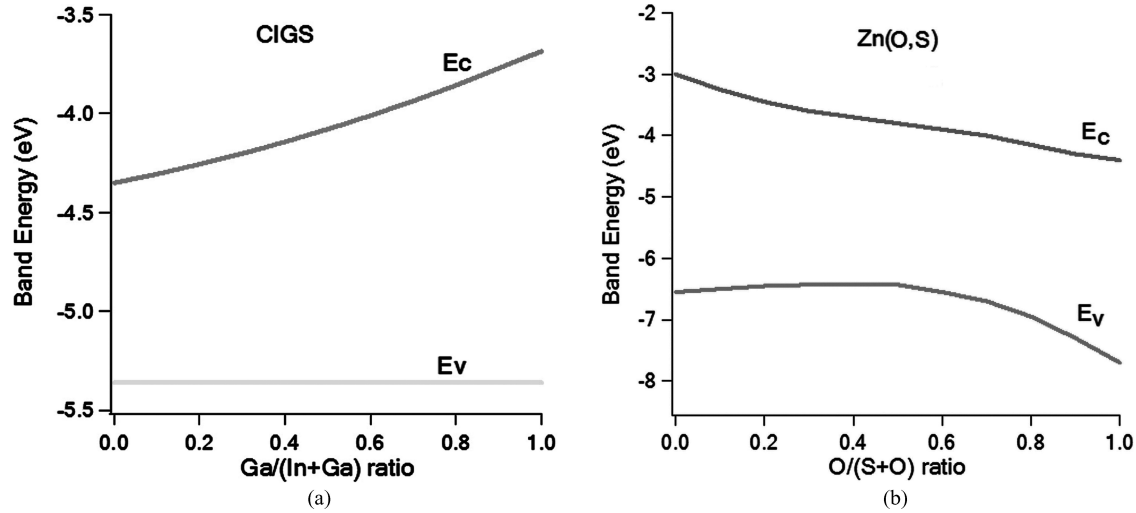

Fig. 1. Energy band diagrams for (a) CIGS as a function of the Ga/(In+Ga) ratio and (b) Zn(O,S) as a function of O/(S+O).

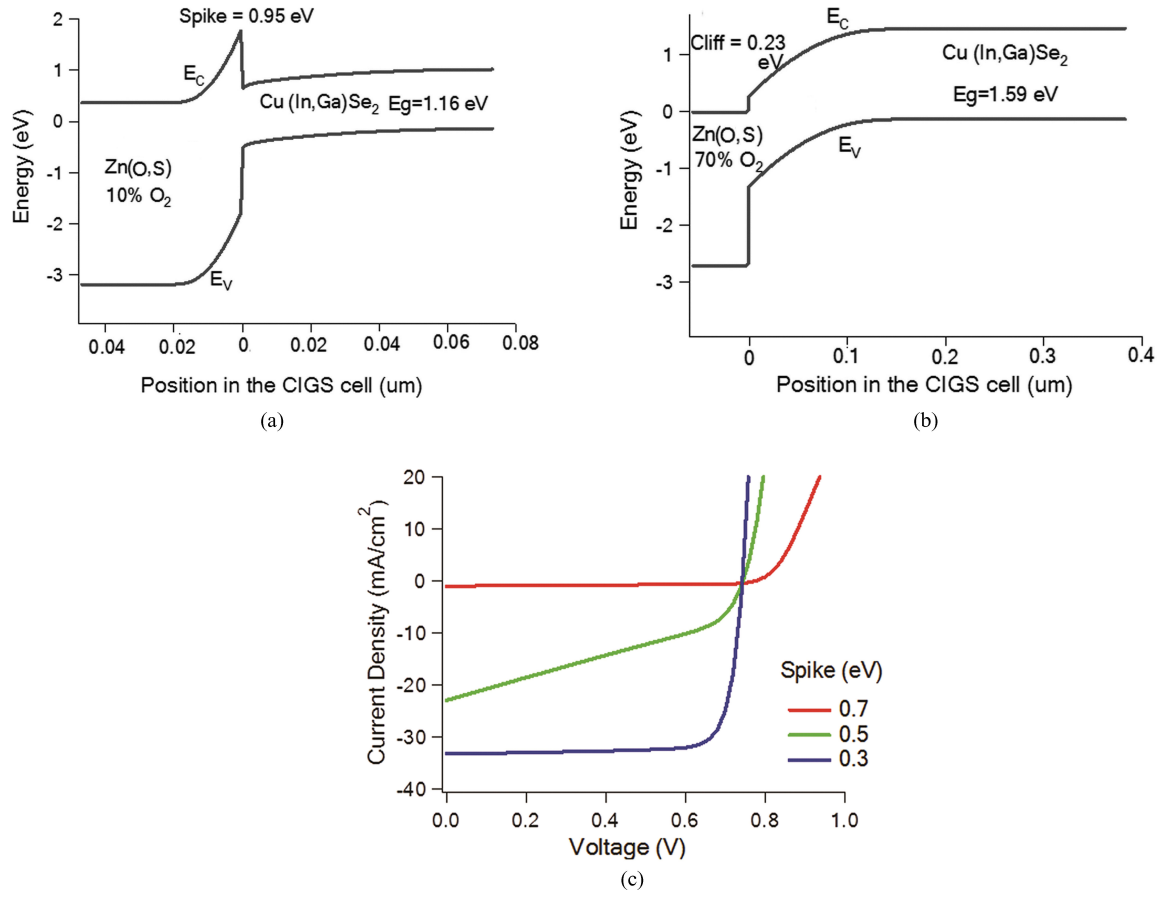

Fig. 2. Band diagram for Zn(O,S)/CIGS cells with (a) 10% O_2 and 30% Ga (large spike) and (b) 70% O_2 and 90% Ga (cliff). (c) $J-V$ curves for positive conduction-band offsets.

III. Band Alignment

The CBO at the interface between Zn(O,S) and CIGS follows directly from Fig. 1. It can range from +1.3 eV for ZnS/CIS to −0.7 eV for ZnO/CGS. A positive offset is depicted in Fig. 2(a) and a negative one in (b). Fig. 2(c), which is dominated by the magnitude of the spike barrier, illustrates the dramatic collapse in photocurrent as the barrier increase limits current flow in forward bias. The current–voltage $(J-V)$ curve for a negative CBO is heavily dependent on the amount of interfacial recombination and will show reductions in the voltage and fill factor resulting from increased forward current. When CdS is used for the buffer layer with CIGS, low gallium concentrations will result in a spike and high ones in a cliff. With Zn(O,S), there is

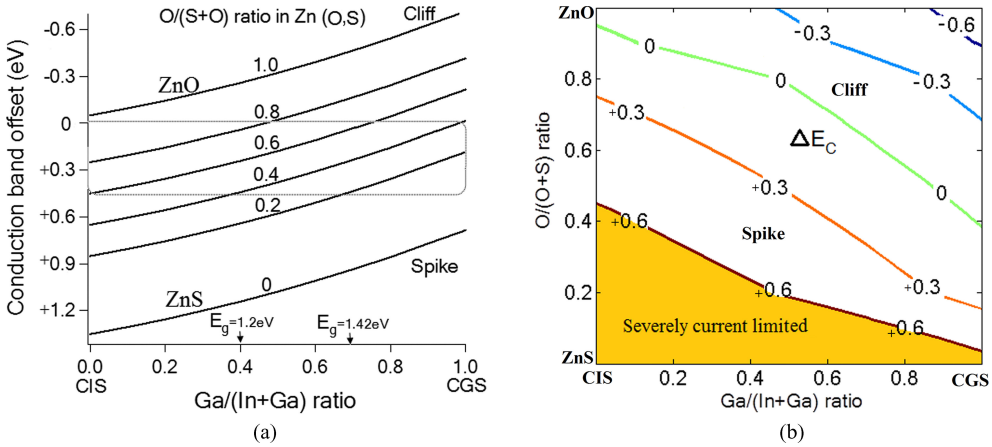

Fig. 3. (a) Calculated conduction band offset for the Zn(O,S)/CIGS heterojunction; the box shows the target range; CdS/CIGS would follow the 0.6 line. (b) Contour plot of CBO (ΔE_C).

a greater range of CBO possibilities, which allows the offset to be tuned to an optimal value for any gallium concentration.

Fig. 3(a) shows the conduction band offset at the Zn(O,S)/CIGS interface for varying amounts of oxygen in Zn(O,S) as a function of CIGS composition. When the buffer is pure ZnS, or has a low oxygen content, the CBO is large and positive for all absorber layers, and the resulting electron barrier is too large to allow any significant current flow. In the opposite direction, larger amounts of oxygen in the buffer layer produce a negative offset, and a fairly substantial one for high gallium concentrations. The dashed box in Fig. 3(a) highlights the ratios where the CBO is between 0 and +0.4 eV, which should include the region of optimal offset. Zn(O,S) with an O/(S+O) ratio of 0.6 should have the same electron affinity as CdS so that line would also correspond to the CBO for CdS/CIGS. Fig. 3(b) shows a contour plot of the same information so that one can track the different combinations of Zn(O,S) and CIGS that yield the same CBO.

IV. Results

Reasonable input parameters for the calculations were based on [23] and were chosen to emulate an 18%-efficient CdS/CIGS cell with a modest level of Ga. Adjustment of the absorption spectra of the two layers for different bandgaps was done by shifting the energy axes of the spectra by the same amount as the bandgap shift; material parameters not directly affected by the bandgap were held constant. Silvaco software [24] was then used to calculate the one-sun room-temperature cell parameters for Zn(O,S)/CIGS: short-circuit current ($J_{\rm SC}$), open-circuit voltage ($V_{\rm OC}$), fill factor (FF), and conversion efficiency for the full range of oxygen and gallium ratios. An important assumption is that the carrier density of the Zn(O,S) is sufficiently high ($\sim 10^{18}$ cm^{-3}) that the TCO/Zn(O,S) CBO does not significantly affect the height of the Zn(O,S)/CIGS spike above the Fermi level [16].

A series of calculated $J-V$ curves for the full range of gallium values is shown in Fig. 4. An oxygen fraction of 0.7 was chosen, because the CBO will transition from a small spike condition to a cliff as the Ga-fraction is increased. Hence, Fig. 4 shows a systematic decrease in current, and it shows that voltage first increases but then saturates at the higher Ga-fractions that correspond to the cliff region.

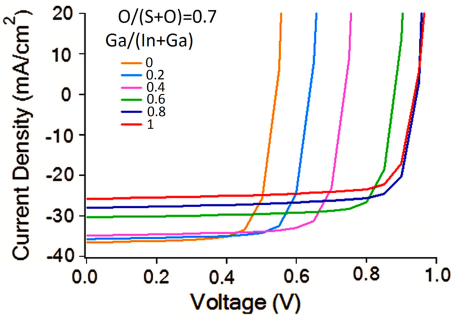

Fig. 4. Calculated J–V curves for full range of Ga content fixed Zn(O,S) oxygen fraction of 0.7.

Calculated values for $J_{\rm SC}$ over the full range of gallium and oxygen values are shown as a contour plot in Fig. 5(a). Over much of the oxygen range, the current decreases with increasing gallium, and hence CIGS bandgap, from about 38 to 25 mA/cm^2. In the high CBO, or low oxygen region, however, the photocurrent is dramatically reduced due to the large spike barrier, as discussed previously. This decrease though is nearly negligible when the CBO smaller than +0.4 eV. The currents in Fig. 5(a), and later the efficiencies, are somewhat higher than for CdS/CIGS with the same offset, because the higher bandgap of Zn(O,S) allows greater collection from short-wavelength photons. The increase over CdS buffer layers has generally been observed in the experimental references cited earlier.

The calculated values for $V_{\rm OC}$ in Fig. 5(b) increase from 500 to 1200 mV as the CIGS bandgap is increased from 1.0 to 1.67 eV. Again there is an exception for the low-oxygen region, where $V_{\rm oc}$ becomes meaningless, because of the extreme limitation on current. Fig. 5(b) also shows that at constant oxygen ratios of 0.6 and above, the voltage saturates as one moves into the cliff region with greater interfacial recombination. This is the voltage saturation shown with the full $J-V$ curves in Fig. 4. The fill-factor dependence in Fig. 5(c) also decreases when one moves away from the +0.3-eV CBO contour in either the spike

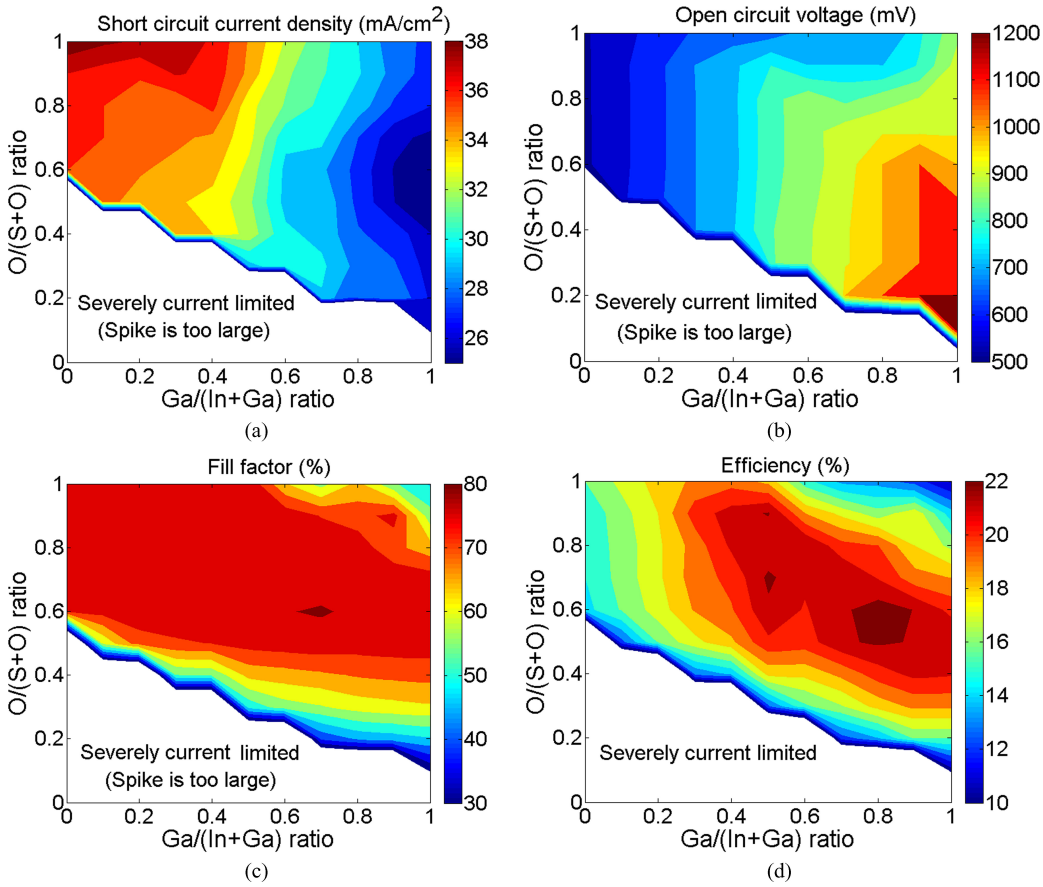

Fig. 5. Calculated contour plots of (a) short-circuit current, (b) open-circuit voltage, (c) fill-factor, and (d) efficiency for Zn(O,S)/CIGS cells as a function of gallium and oxygen fractions.

or the cliff direction, as one would expect from the earlier discussion. Near the preferred CBO contour, however, the fill-factor is relatively constant at about 75% for the parameters used.

The room-temprature efficiency contour plot in Fig. 5(d) is the product of the other three. If one follows the prefered CBO contour from Fig. 3(b) with increasing gallium, the efficiency increases by several percent from pure CIS, then changes very little over a broad plateau, and then decreases slightly as one approaches CGS. Again, there will lower efficiency on either side of the preferred CBO contour.

Since a primary argument for a higher bandgap absorber is a lower temperature coefficient for voltage and efficiency, the calculations were repeated for a temperature of 60 °C, and the higher temperature efficiency contours are shown in Fig. 6(a). The primary change is in the cell voltage, which decreases with increasing temperature at approximately −2 mV/K, which means a smaller percentage increase at higher volatages generated by higher gallium and bandgap. The fill factor at higher temperature weakly tracks the voltage decrease, and the current is essentially unchanged. The efficiency contours in Fig. 6(a) are lower over most of the plane, except in the lower oxygen region, where a slightly higher CBO spike can be tolerated at higher temperatures. As a consequence, the white region of severely limited current is somewhat smaller. Of practical interest is the efficiency difference between higher and lower temperatures, which is shown in Fig. 6(b). Along the preferred-CBO contour from Fig. 3(b), the efficiency loss between 25 °C and 60 °C varies from over 2% for CIS at the left to less than 1% for CGS at the right.

V. Discussion

Results from any simulation are obviously sensitive to the choice of parameters used, and it is useful to ask whether Figs. 4–6 would be significantly altered if the parameters were varied. The severe current limitation with the large spike should be relatively insensitive to the details, but a modest spike could be accentuated for the combinations of low-carrier-density and relatively thick buffer layers [16], and the result could be distortions in the current–voltage curves that reduce the fill factor. The cliff direction is also sensitive to parameter choice, in this case the degree of interfacial recombination. If the recombination is small, the cliff will have relatively little impact on cell performance. Other parameters that primarily affect current are set by experimental considerations and do not have a direct impact on voltage and fill factor.

CIGS absorbers often have a composition grading due to gallium accumulation toward the back of the absorber or, in some cases, modest bandgap expansion at the front as well. Compositional grading is not addressed here, but the electron affinity

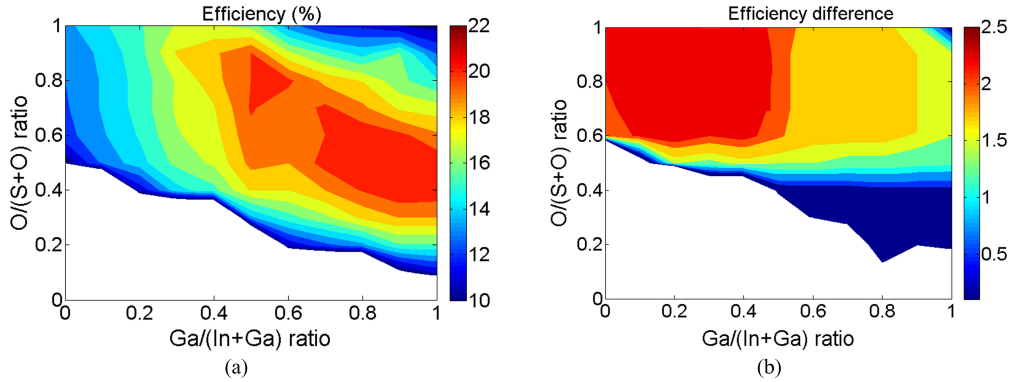

Fig. 6. (a) Efficiency contours at 60 °C. (b) Efficiency loss between 25 °C and 60 °C.

near the buffer interface should be the relevant parameter. Another question is whether one can extend the results shown here to a similar absorber, such as CIGS alloyed with sulfur or silver, or to the kesterites. The general principles should apply, but the utility of Zn(O,S) for the buffer, and the ability to vary its electron affinity, will depend on the absorber's electron affinity and whether there is significant change in it when its alloy ratio is changed. In general, one would expect absorber alloys with anion alterations to have less change in their electron affinity than those with cation variations.

VI. Conclusion

The optimal band-alignment match between a Zn(O,S) buffer and CIGS absorber depends critically on the oxygen and gallium ratios. There is more flexibility with a Zn(O,S) buffer than with CdS to optimize the alignment, but because of the complex nature of how the Zn(O,S) bands vary with oxygen composition, it is more difficult to determine the optimal composition for the full range of CIGS. Calculations here show that the target oxygen composition at room temperature based on band-offset considerations alone should decrease from above 90% for CIS to approximately 50% for CGS. For CIGS with a bandgap near the optimal 1.4 eV, the Zn(O,S) buffer should have 60% to 70% oxygen. At higher temperatures, there is negligible change in the target for the oxygen ratio, but as one expects in general, the efficiency decrease is less when higher bandgap CIGS is used.

References

[1] T. Nakada and M. Mizutani, "Improved efficiency of Cu(In,Ga)Se_2 thin film solar cells with chemically deposited ZnS buffer layers by air annealing formation of homojunction by solid phase diffusion," in *Proc. 28th IEEE Photovoltaic Spec. Conf.*, Anchorage, AK, USA, Sep. 2002, pp. 529–534.

[2] T. Nakada, M. Mizutani, Y. Hagiwara, and A. Kunioka, "High-efficiency Cu(In,Ga)Se_2 thin-film solar cells with a CBD-ZnS buffer layer," *Sol. Energy Mater. Sol. Cells*, vol. 67, pp. 255–260, 2001.

[3] Y.-Z. Yoo, Z.-W. Jin, T. Chikyow, T. Fukumura, M. Kawasaki, and H. Koinuma, "S doping in ZnO film by supplying ZnS species with pulsed laser deposition method," *Appl. Phys. Lett.*, vol. 81, p. 3798, 2002.

[4] B. K. Meyer, A. Polity, B. Farangis, Y. He, D. Hasselkamp, T. Kramer, C. Wang, U. Haboeck, and A. Hoffmann, "On the composition dependence of $ZnO_{1-x}S_x$," *Phys. Status Solidi C*, vol. 1, p. 694, 2004.

[5] A. Okamoto, T. Minemoto, and H. Takakura, "Application of sputtered $ZnO_{1-x}S_x$ buffer layers for Cu(In,Ga)Se_2 solar cells," *Jpn. J. Appl. Phys.*, vol. 50, p. 04DP10, 2011.

[6] D. Hariskos, R. Menner, P. Jackson, S. Paetel, W. Witte, W. Wischmann, M. Powalla, L. Bukert, T. Kolb, M. Oertel, B. Dimmler, and B. Fuchs, "New reaction kinetics for a high-rate chemical bath deposition of the Zn(S,O) buffer layer for Cu(In,Ga)Se_2-based solar cells," *Prog. Photovolt., Res. Appl.*, vol. 20, pp. 534–542, 2012.

[7] C. Platzer-Bjorkman, T. Torndahl, D. Abou-Ras, J. Malmstrom, J. Kessler, and L. Stolt, "Cu(In,Ga)Se_2/Zn(O,S) solar cells: Band alignment and sulfur gradient," *J. Appl. Phys.*, vol. 100, pp. 044506-1–044506-9, 2006.

[8] K. Ramanathan, J. Mann, S. Glynn, S. Christensen, J. Pankow, J. Li, J. Scharf, L. Mansfield, M. Contreras, and R. Noufi, "Comparative study of Zn(O,S) buffer layers and CIGS solar cells fabricated by CBD, ALD, and sputtering," in *Proc. 38th IEEE Photovoltaic Spec. Conf.*, Austin, TX, USA, Jun., 2012.

[9] A. O. Pudov, J. R. Sites, and T. Nakada, "Performance and loss analyses of high-efficiency chemical bath deposition (CBD)-ZnS/Cu($In_{1-x}Ga_x$)Se_2 thin-film solar cells," *Jpn. J. Appl. Phys.*, vol. 41, pp. L672–L674, 2002.

[10] A. Ennaoui, S. Siebentritt, M. C. Lux-Steiner, W. Riedl, and F. Karg, "High-efficiency Cd-free CIGSS thin-film solar cells with solution grown zinc compound buffer layers," *Sol. Energy Mater. Sol. Cells*, vol. 67, pp. 31–40, 2001.

[11] T. Nakada, "18% efficiency Cd-Free Cu(In, Ga)Se_2 thin-film solar cells fabricated using chemical bath deposition (CBD)-ZnS buffer layers," *Jpn. J. Appl. Phys.*, vol. 41, pp. L165–L167, 2002.

[12] K. Kushiya, M. Tachiyuki, Y. Nagoya, A. Fujimaki, B. Sang, D. Okumura, M. Satoh, and O. Yamase, "Progress in large-area Cu(InGa)Se_2-based thin-film modules with a Zn(O,S,OH)$_x$ buffer layer," *Sol. Energy Mater. Sol. Cells*, vol. 67, p. 11, 2001.

[13] H. Muffler, M. Bär, C. Fisher, R. Gay, F. Karg, and M. Lux-Steiner, "IIgar technology, VIII: Sulfidic buffer layers for Cu(In,Ga)(Se,S)$_2$ solar cells prepared by ion layer gas reaction (Ilgar)," in *Proc. 29th IEEE Photovoltaics Spec. Conf.*, New Orleans, LA, USA, May 2002, pp. 610–613.

[14] M. Gloeckler and J. R. Sites, "Efficiency limitations for wide-band-gap chalcopyrite solar cells," *Thin Solid Films*, vol. 480–481, pp. 241–245, 2005.

[15] A. O. Pudov, M. A. Contreras, T. Nakada, H.-W. Schock, and J. R. Sites, "CIGS J-V distortions in the absence of blue photons," *Thin Solid Films*, vol. 480–481, pp. 273–278, 2005.

[16] A. O. Pudov, F. S. Hasoon, A. Kanevce, H. Al-Thani, and J. R. Sites, "Secondary barriers in CdS-$CuIn_{1-x}Ga_xSe_2$ Solar Cells," *J. Appl. Physics*, vol. 97, p. 064901, 2005.

[17] M. Gloeckler, "Device physics of Cu(In,Ga)Se_2 thin-film solar cells," Ph.D. dissertation, Colorado State Univ., Fort Collins, CO, USA, 2005.

[18] T. Minemoto, T. Matsui, H. Takakura, Y. Hamakawa, T. Negami, Y. Hashimoto, T. Uenoyama, and M. Kitagawa, "Theoretical analysis of the effect of conduction band offset of window/CIS layers on performance of CIS solar cells using device simulation," *Sol. Energy Mater. Sol. Cells*, vol. 67, pp. 83–88, 2001.

[19] S. Wei and A. Zunger, "Calculated natural band offsets of all IIVI and IIIV semiconductors: Chemical trends and the role of cation d orbitals," *Appl. Phys. Lett.*, vol. 72, p. 2011, 1998.

[20] T. Minemoto, A. Okamoto, and H. Takakura, "Sputtered ZnO-based buffer layer for band offset control in Cu(In,Ga)Se_2 solar cells," *Thin Solid Films*, vol. 519, pp. 7568–7571, 2011.

[21] B. K. Meyer, A. Polity, B. Farangis, Y. He, D. Hasselkamp, T. Kramer, and C. Wang, "Structural properties and bandgap bowing of $ZnO_{1-x}S_x$

thin films deposited by reactive sputtering," *Appl. Phys. Lett.*, vol. 85, p. 4929, 2004.
[22] A. Grimm, D. Kieven, R. Klenk, I. Lauermann, A. Neisser, T. Niesen, and J. Palm, "Junction formation in chalcopyrite solar cells by sputtered wide gap compound semiconductors," *Thin Solid Films*, vol. 520, p. 1330, 2011.
[23] M. Gloecker, A. Fahrenbruch, and J. Sites, "Numerical modeling of CIGS and CdTe solar cells: Setting the baseline," in *Proc. 3rd World Conf. Photovoltaic Energy Convers.*, Osaka, Japan, 2003, pp. 491–494.
[24] Silvaco ATLAS Device Simulator. (2012). [Online]. Available: http://www.gobookee.net/silvaco-solar-cell/

Samaneh Sharbati received the B.Sc. and M.S. degrees in electronic engineering from Semnan University, Semnan, Iran, in 2001 and 2006, respectively. She joined the Device Simulation and Modeling Group of Tehran University for two years. She is currently working toward the Ph.D. degree in electrical engineering with the Ferdowsi University of Mashhad, Mashhad, Iran.

In 2013, she was a Visiting Scholar with the Department of Physics, Colorado State University, Fort Collins, CO, USA.

James R. Sites received the B.S. degree from Duke University, Durham, NC, USA, in 1965 and the Ph.D. from Cornell University, Ithaca, NY, USA, in 1969.

Since 1971, he has been with Colorado State University (CSU), Fort Collins, CO, USA, where he is currently the Senior Associate Dean for Research with the College of Natural Sciences. From 1990 to 2000, he served as Chair of the Physics Department at CSU.